NEW RESULTS ON CHARM PRODUCTION AT HERA*

Uri Karshon

on behalf of the H1 and ZEUS collaborations

Weizmann Institute of Science, 234 Herzl Street, Rehovot 7610001, Israel

(Received May 26, 2014)

The copious production of charm quarks at HERA yielded measurements of the charm contribution to the proton structure and of the charm mass and fragmentation parameters of charmed hadrons. Several measurements of charm production in deep inelastic scattering from the H1 and ZEUS collaborations as well as combined data are presented. They provide a powerful vindication of the form of the gluon density in the proton derived from scaling violations of inclusive deep inelastic scattering data. A QCD fit to the charm data leads to a measurement of the charm mass and provides precise predictions *e.g.* for W and Z production at the LHC. In addition, charm fragmentation fractions in photoproduction to ground state charm hadrons are compared to e^+e^- data and support the hypothesis of fragmentation independence of the production process.

DOI:10.5506/APhysPolBSupp.7.511
PACS numbers: 13.60.Le, 14.40.Lb, 14.65.Dw

1. Introduction

Production of the ground-state charm mesons D and D^* was extensively studied at the HERA ep collider. Since the charm quark coupling to a photon is stronger than the down-quarks (d, s, b), the charm production cross section is large. Two kinematic regimes exist at HERA: Photoproduction (PHP) with $Q^2 \approx 0$, where the scattered electron is undetected, and Deep Inelastic Scattering (DIS) with $Q^2 >$ few GeV^2, where the scattered electron is detected. Here, Q^2 is the exchanged photon virtuality. The charm contribution to inclusive DIS cross section at HERA is up to 30%. The dominant process for charm production in DIS is boson–gluon fusion, where a gluon from the proton interacts with the photon, W or Z from the incoming electron. Thus, this process is a direct probe of the gluon density in the proton.

* Presented at "Excited QCD 2014", Bjelašnica Mountain, Sarajevo, Bosnia and Herzegovina, February 2–8, 2014.

It is also sensitive to the charm quark mass, m_c, and enables testing QCD by comparing data to next-to-leading (NLO) predictions. Multiple scales in this process (Q^2, m_c and transverse momentum of the charm quark) allow perturbative calculations. The charm contribution to the proton structure function, F_2, can be extracted. Fractions of charm quarks hadronising to charm hadrons can test the universality of the fragmentation fractions.

The HERA *ep* collider operated with electrons or positrons at 27.5 GeV and protons at 820 or 920 GeV. About 126 pb^{-1} of data was taken between 1995–2000 (HERA I) and ≈ 373 pb^{-1} was taken between 2003–2007 (HERA II) by each of the two main general experiments H1 and ZEUS.

2. Theory of charm quark production

Several NLO schemes for charm production in *ep* collisions exist:

(1) "Massive" or Fixed Flavour Number Scheme (FFNS), where $Q^2 \approx m_c^2$. In this scheme only three active flavours (u, d, s) in the proton are considered, the charm quark is produced only perturbatively in the hard scattering and mass effects are correctly included.

(2) "Massless" or Zero-Mass Variable Flavour Number Scheme (ZM-VFNS), where $Q^2 \gg m_c^2$. Here, charm is treated as a massless parton, the charm density is added as a fourth flavour in the proton and a resummation of large logarithms of Q^2/m_c^2 is performed.

At intermediate Q^2 both schemes should be merged:

(3) General-Mass Variable Flavour Number Scheme (GM-VFNS). This scheme is equivalent to FFNS for $Q^2 < m_c^2$ and to ZM-VFNS for $Q^2 > m_c^2$. In between, various schemes interpolate differently from each other.

3. $D^{\pm}$ and $D^{*\pm}$ production in deep inelastic scattering

$D^{\pm}$ and $D^{*\pm}$ production has been studied by ZEUS in DIS [1, 2] with the full HERA II data. Clean signals of 8356 ± 198 D^+ events in the $M(K^-\pi^+\pi^+)$ distribution and 12893 ± 185 D^{*+} events in the $M(K^-\pi^+\pi^+) - M(K^-\pi^+)$ distribution were seen. (Charge-conjugate states are included.) In Fig. 1 D^+ differential cross sections are given w.r.t. $Q^2, y, p_{\mathrm{T}}(D^+), \eta(D^+)$ in the kinematic region $5 < Q^2 < 1000$ GeV^2, $1.5 < p_{\mathrm{T}}(D^+) < 15$ GeV, $|\eta(D^+)| < 1.6$, $0.02 < y < 0.7$. Here, $y = Q^2/(sx)$, where s is the total energy squared of the *ep* system, x is the Bjorken variable and $p_{\mathrm{T}}(D^+)$ and $\eta(D^+)$ are, respectively, the D^+ transverse momentum and pseudorapidity. NLO predictions based on FFNS describe the data well. D^{*+} differential cross sections w.r.t. $Q^2, y, x, p_{\mathrm{T}}(D^{*+}), \eta(D^{*+})$ in the kinematic

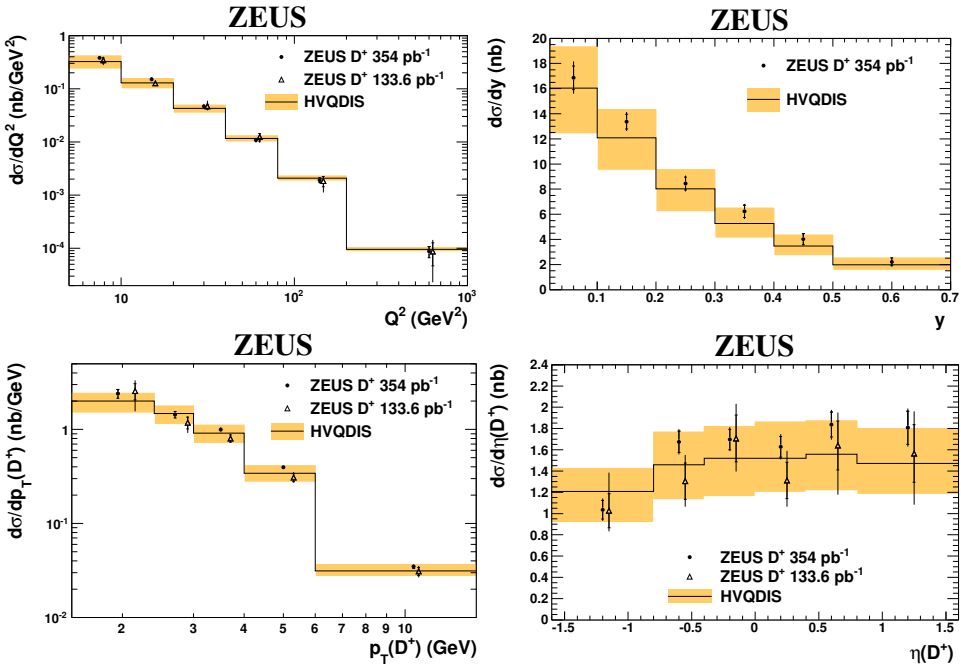

Fig. 1. D^+ differential cross sections as a function of $Q^2, y, p_{\mathrm{T}}(D^+), \eta(D^+)$. Solid lines and shaded bands are NLO FFNS predictions.

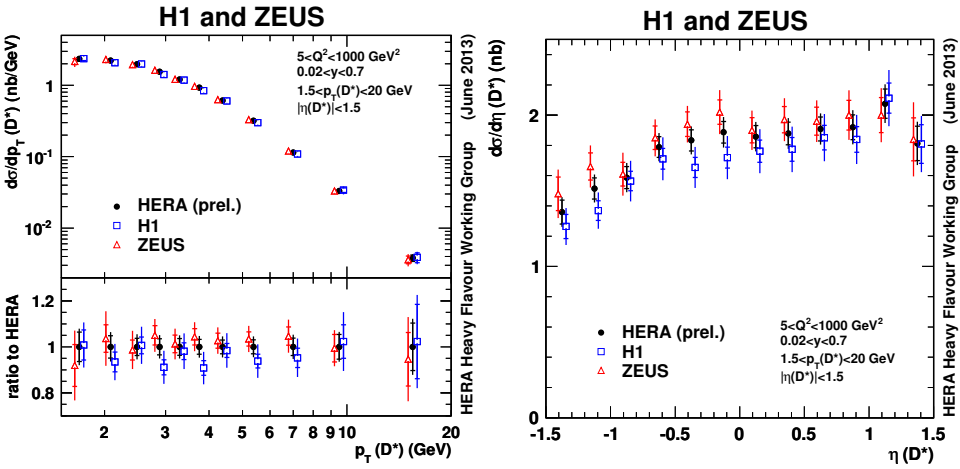

Fig. 2. Combined H1+ZEUS D^* differential cross sections as a function of $p_{\mathrm{T}}(D^*), \eta(D^*)$.

region $5 < Q^2 < 1000$ GeV^2, $1.5 < p_{\mathrm{T}}(D^{*+}) < 20$ GeV, $|\eta(D^{*+})| < 1.5$, $0.02 < y < 0.7$ (not shown) are also described well by NLO predictions based on FFNS. In Fig. 2 combined H1+ZEUS differential cross sections w.r.t. $p_{\mathrm{T}}(D^{*+}), \eta(D^{*+})$ are shown with all relevant correlations taken into account [3]. The uncertainties are strongly reduced in the combined results.

The charm reduced cross section $\sigma_{\mathrm{red}}^{c\bar{c}}$ can be defined as $F_2^{c\bar{c}} - \frac{y^2}{Y_+} F_L^{c\bar{c}}$, where $F_2^{c\bar{c}}, F_L^{c\bar{c}}$ are the charm contributions to the proton structure functions F_2 and F_L and $Y_+ = 1+(1-y)^2$. In Fig. 3 $\sigma_{\mathrm{red}}^{c\bar{c}}$ is shown as a function of x for various Q^2 values. In the left plot, ZEUS results are shown for D^+ and D^{*+} and combined H1+ZEUS results are given for D^{*+}. All measurements are in good agreement with each other. In the right plot, the ZEUS D^{*+} results are compared to the GM-VFNS predictions. The predictions describe well the new precise data.

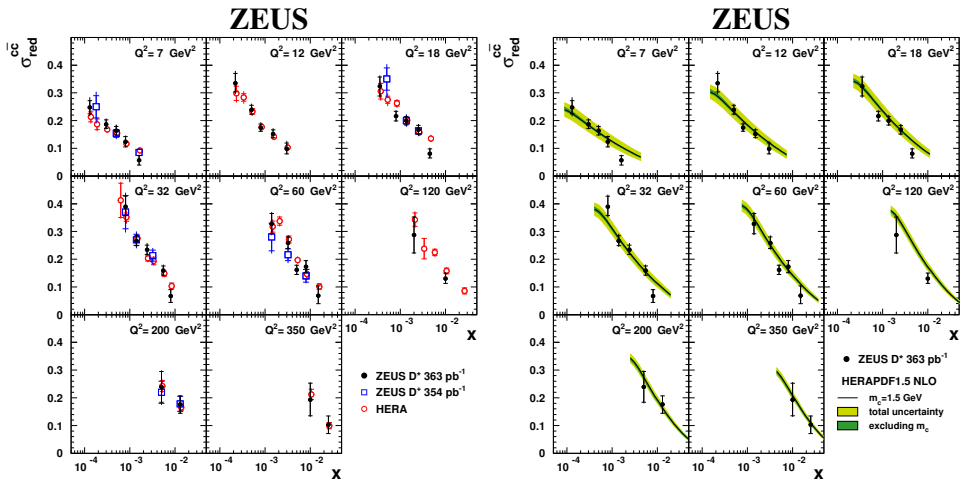

Fig. 3. $\sigma_{\mathrm{red}}^{c\bar{c}}$ for D^+ and D^{*+} from ZEUS and for D^{*+} from H1+ZEUS as a function of x for various Q^2 values (left plot). In the right plots, the ZEUS D^{*+} results are compared to the predictions of GM-VFNS.

4. Charm fragmentation fractions in photoproduction

The probability of a c quark to hadronise into a given charm hadron (fragmentation fraction) was measured in the PHP regime for the D^0, D^+, D^{*+}, D_s, Λ_c hadrons [4]. The results shown in Fig. 4 (left column) are compared with previous results. The precision is competitive with the combined e^+e^- results (right column). The fragmentation fractions are found to be independent of the production mechanism, supporting the hypothesis of universality of heavy-quark fragmentation.

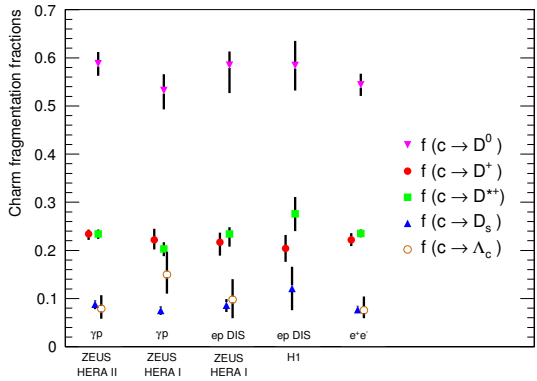

Fig. 4. Fragmentation fractions of c quarks hadronising to the charm hadrons $D^0, D^+, D^{*+}, D_s, \Lambda_c$ in PHP (left column) compared to previous results.

5. HERA charm data combination in deep inelastic scattering

Charm DIS production cross sections of H1 and ZEUS from various HERA I and HERA II analyses were combined [5]. Reduced cross sections, $\sigma_{\rm red}^{c\bar{c}}$, were obtained in the kinematic range $2.5 < Q^2 < 2000$ GeV^2, $3.10^{-5} < x < 5.10^{-2}$. The charm mass in GM-VFNS was treated as an effective mass parameter M_c. Different optimal M_c values are obtained in various schemes.

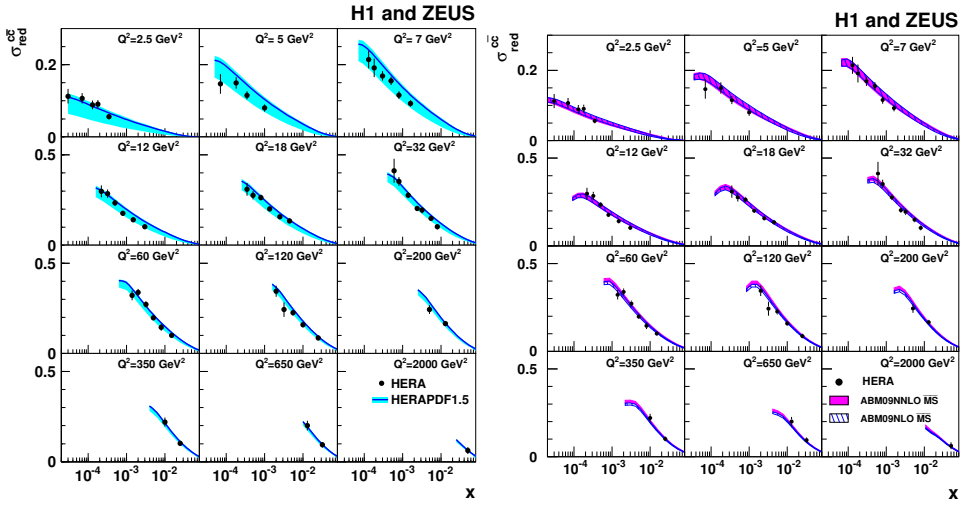

Fig. 5. $\sigma_{\rm red}^{c\bar{c}}$ from H1+ZEUS as a function of x for various Q^2 values. Combined inclusive DIS data are compared to GM-VFNS (left plot). The lines are predictions with $M_c = 1.4$ GeV. In the right plot, the combined charm data are compared to one of the FFNS schemes.

In Fig. 5 $\sigma_{\rm red}^{c\bar{c}}$ is plotted as a function of x for fixed Q^2 values. In the left plot, the data are compared to one of the GM-VFNS schemes. The large theory uncertainties are dominated by the M_c variation. In the right plot, the data are compared to one of the FFNS schemes. In both cases, the theory describes the data well.

NLO analysis is performed using $\sigma_{\rm red}^{c\bar{c}}$ with combined inclusive DIS cross sections in the kinematic range $W > 15$ GeV, $x < 0.65$, $Q^2 > 3.5$ GeV^2. Here W is the γp CM energy. For each NLO scheme, fits are performed with $1.2 < M_c < 1.8$ GeV. For each fit, $\chi^2(M_c)$ is calculated and $M_c^{\rm opt}$ is determined from a parabolic fit (Fig. 6, left). Clear minimal χ^2 values are seen for each scheme at a different $M_c^{\rm opt}$. The data are described much better with $M_c^{\rm opt}$ than with fixed M_c and the predictions of all schemes are similar for $Q^2 > 5$ GeV^2 (Fig. 6, right).

This analysis has interesting implications on NLO predictions for W and Z production at the LHC: The W and Z cross sections for LHC at $\sqrt{s} = 7$ TeV have been calculated for each scheme for $1.2 < M_c < 1.8$ GeV in 0.1 GeV steps (not shown). All cross sections rise monotonically with M_c. Significant spread of $\approx 6\%$ is seen between the predictions for any fixed M_c which reduces to $\approx 1.4{-}2\%$ when taking $M_c^{\rm opt}$ for each scheme.

A global QCD fit of charm and inclusive DIS data has been performed using a NLO analysis in the FFNS scheme. Using the same χ^2 minimization procedure as for the VFNS analysis, the charm running mass $m_c(m_c) = 1.26 \pm 0.05_{\rm exp} \pm 0.03_{\rm mod} \pm 0.02_{\rm param} \pm 0.02_{\alpha_s}$ GeV has been extracted. The errors are experimental, model, parametrization and α_s, respectively. This result is consistent with the PDG one: $m_c(m_c) = 1.275 \pm 0.025$ GeV.

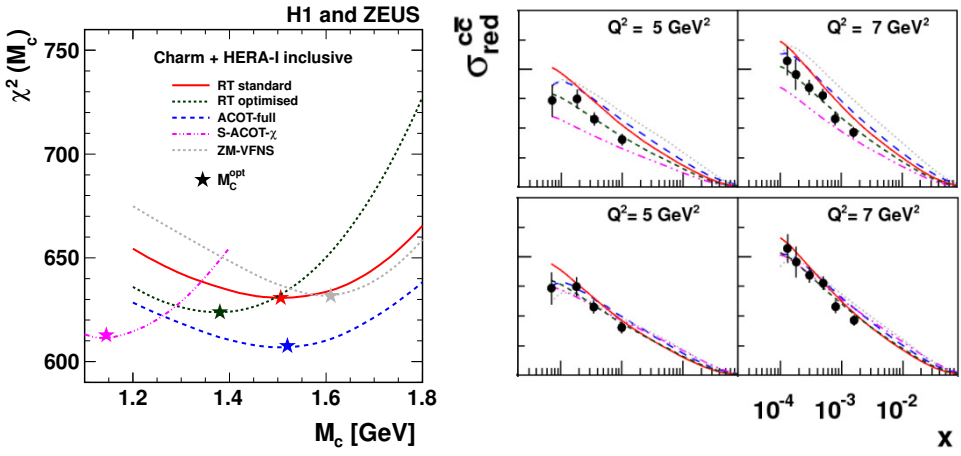

Fig. 6. Left: χ^2 values from fits for various heavy flavour schemes. Right: VFNS predictions for $\sigma_{\rm red}^{c\bar{c}}$ with $M_c = 1.4$ GeV (up) and $M_c = M_c^{\rm opt}$ (down).

REFERENCES

[1] H. Abramowicz *et al.* [ZEUS Collaboration], *J. High Energy Phys.* **05**, 023 (2013).

[2] H. Abramowicz *et al.* [ZEUS Collaboration], *J. High Energy Phys.* **05**, 097 (2013).

[3] H1+ZEUS collaborations, H1prelim-13-171, ZEUSprelim-13-002, 2013.

[4] H. Abramowicz *et al.* [ZEUS Collaboration], *J. High Energy Phys.* **09**, 058 (2013).

[5] H. Abramowicz *et al.* [H1+ZEUS collaborations], *Eur. Phys. J.* **C73**, 2311 (2013).